Optimization of a flatbed scanner acquisition and sample presentation parameters for sugar color measurement: comparison with spectrophotometry; a case study

Leila Ziafar, Keivan Ansari, Masoud Honarvar, Vahid Mohammadi

Optimization of a Flatbed Scanner Acquisition and Sample Presentation Parameters for Sugar Color Measurement: Comparison with Spectrophotometry; A case study

Leila Ziafar [1], Keivan Ansari [2,*], Masoud Honarvar [1], Vahid Mohammadi [3]

[1] Department of Food Science and Technology, SR.C, Islamic Azad University، Tehran, Iran
[2] Department of Color Imaging and Color Image Processing, Institute for Color Science and Technology, Tehran, Iran
[3] IMVIA, Université Bourgogne Europe, UR 7535, 21000 Dijon, France

* Corresponding author. Department of Color Imaging and Color Image Processing, Institute for Color Science and Technology, Tehran, Iran
E-mail address: kansari@icrc.ac.ir (K. Ansari).

Abstract

Accurate color measurement is essential for quality control in white powdered foods such as sugar. While spectrophotometers are the reference instruments, their cost limits routine use in resource limited settings. Flatbed scanners provide an affordable alternative, but their accuracy depends strongly on technical settings and sample presentation. This study systematically optimized a commercial flatbed scanner parameters (power supply, gamma correction, internal color management, image format, bit depth, and resolution) and physical variables (container dimensions, cover type, and substrate) for a sugar sample color measurement. Spectrophotometric measurements (D_{65} illuminant, 2° observer) served as the reference, and color differences were quantified using ΔE_{00}. Images captured via an Epson flatbed scanner were processed to derive mean RGB values. Results show that operating the scanner under mains power, using manual gamma correction ($\gamma = 2.2$), 24-bit TIFF format, and 300 dpi resolution, minimized the color difference to $\Delta E_{00} \approx 4.07$, significantly improving accuracy compared to internal color management profiles ($\Delta E_{00} \approx 6.9 – 7.2$). Increasing bit depth to 48-bit or resolution beyond 300 dpi yielded negligible gains. Physically, a non-fluorescent white cover, quartz substrate, and sample container diameter ≥ 4 cm further improved repeatability. Three way ANOVA confirmed significant interactions ($p<0.001$) between cover type and diameter. The study concludes that while the scanner does not yet meet strict industrial tolerances ($\Delta E_{00} <2$), it provides a repeatable and cost-effective alternative for relative color measurement quality screening of white powdered foods when proper optimization protocols are followed in resource-limited settings.

Keywords: Sugar; Scanner; Spectrophotometer; Image processing; Color measurement;

1. Introduction

Color is a key quality measurement attribute in white powdered foods such as sugar, influencing both process control and consumer acceptance [1-3]. Spectrophotometers are considered the reference instruments for color measurement, yet their high cost and maintenance requirements can limit routine use in many laboratories [4-6]. In contrast, digital flatbed scanners are inexpensive, widely available devices that can capture high-resolution RGB images and therefore represent an attractive alternative for objective color assessment in food product quality measurement [7,8].

However, commercial scanners are not designed as colorimetric instruments. Their output depends on internal light sources, sensor characteristics, embedded image processing and color management, as well as software settings selected by the user [9-11]. As a result, raw scanner RGB values cannot be directly compared with standard color spaces such as CIELAB without proper characterization and control of acquisition conditions [12]. Previous work on scanner characterization and imaging systems has mostly focused on graphic arts, medical or dental

applications, and often considers only a subset of technical factors such as color space, gamma correction or resolution [13]. In the context of powdered food materials, the combined effects of scanner settings and sample presentation on achievable color accuracy remain insufficiently studied. While flatbed scanners have been characterized for opaque foods, their application to crystalline, semi-translucent powders like sugar has been limited by the complex subsurface scattering of light. This study provides the first systematic optimization of scanner acquisition parameters specifically tailored to overcome the optical challenges of white powdered matrices.

For powdered food samples like sugar, both the device configuration and the physical arrangement of the sample can alter the recorded RGB values. Technical parameters include the power supply stability, internal color management profile, gamma correction, output image format, bit depth and spatial resolution. Physical and optical factors include the properties of the container (height and diameter), whether the transparent cover holding the sugar sample is white or black, whether the presence of fluorescent materials affects the results, and the nature of the transparent substrate between the sample and scanner glass. These variables influence light distribution, scattering paths and sensor responses, and therefore must be optimized if flatbed scanners are to serve as reliable color measurement tools [14]. Unlike opaque materials, crystalline powders such as sugar are partially translucent, allowing light to pass through the particles rather than reflecting only from the surface. When the sample is illuminated, light can enter the crystals, scatter internally, and reach the substrate below before returning to the sensor. This means that the captured color depends not only on the powder itself but also on the optical properties of the surface substrate, such as its transparency and reflectivity. Because flatbed scanners are designed for opaque documents, standard scanner settings often fail to capture the true color of crystalline powders unless the substrate effect is carefully controlled.

The objective of this study was to systematically evaluate the influence of technical and physical factors on scanner-based color measurements for a white powdered sugar sample, using spectrophotometric data as a reference. We examined the effects of power source, gamma correction, internal color management, image format, bit depth and resolution, together with container height and diameter, cover type and substrate. For each condition, scanner-derived RGB values were converted to CIELAB coordinates and compared with spectrophotometer measurements under the D_{65} illuminant and 2° observer geometry via ΔE_{00} and ΔE^{*}_{ab} indices.

By identifying a combination of scanner settings and sample preparation conditions that minimize the color difference relative to the spectrophotometer, this work provides a practical optimization protocol for using a flatbed scanner as an accessible, low-cost colorimetric device for white powdered food materials such as sugar. The approach may be extended to other powder systems with different scattering and absorption properties.

2. Materials and Methods

For this study, one commercial white sugar sample (Grade 1) was randomly selected from various samples obtained from Qazvin Sugar Factory, compliant with national standard ISIRI 69 and international standard Codex Stan 212. These standards strictly regulate particle size distribution (Mean Aperture 0.5 - 0.6 mm, CV < 30%) and moisture content (<0.04%), thereby ensuring the sample represents the standardized optical texture of industrial sugar production[15-17].

The sample was transferred and analyzed in a lab under dark, humidity-controlled conditions. A MINOLTA-CS2000 spectrophotometer measured the sample's spectral reflectance (1 cm aperture, 45°/0° geometry; figure 1). XYZ and $L^{*}a^{*}b^{*}$ color values were then determined under 2-degree and D_{65} observer/illuminant standard conditions [18, 19]. An EPSON V700 PHOTO flatbed scanner captured images, which were circularly cropped (figure 2). Image acquisition was performed using the Epson Scan utility (version 3.9.2.2) operating in Professional Mode. This configuration allowed for the manual specification of all scanning parameters, ensuring that no automatic image adjustments were applied during the process. Before starting the measurements, the scanner was kept on for 15 minutes to ensure stable measurement conditions. Average RGB data from these images were converted to XYZ and $L^{*}a^{*}b^{*}$ color values using specific transfer matrices [20,21]. All calculations were performed using MATLAB 2023b.

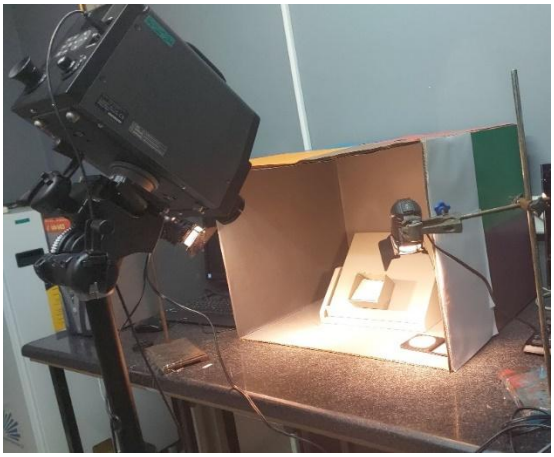

Figure 1. Geometry of spectral reflectance measurement using the spectrophotoradiometer.

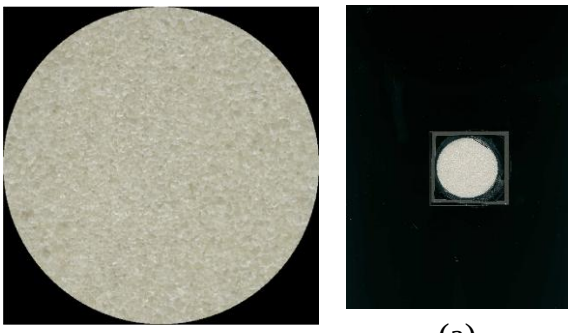

Figure 2. Scanned sugar sample images: (a) before cropping; (b) after cropping.

Table 1 details the color values of sugar samples, while figure 3 displays their spectral reflectance curves, derived from five spectrophotometer measurements. These results confirm the high accuracy of spectrophotometer-based reflectance curve measurement.

Table 1. Five replicate spectrophotoradiometer measurements of sugar sample color values.

	L^*	a^*	b^*	C^*	h°
1	74.18	1.73	12.42	12.54	82.05
2	74.17	1.73	12.43	12.54	82.09
3	74.18	1.72	12.43	12.54	82.11
4	74.19	1.72	12.42	12.54	82.1
5	74.2	1.72	12.43	12.55	82.12
AVE	74.18	1.72	12.43	12.54	82.09
STD	0.0114	0.0055	0.0055	0.0045	0.0270

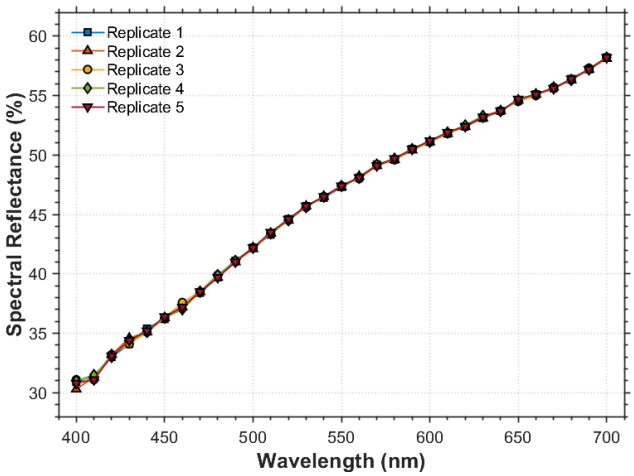

Figure 3. Five spectral reflectance curves measured by the spectrophotometer (five replicates).

To establish a robust acquisition protocol, specific technical and physical variables affecting scanner performance were systematically isolated based on known optical principles. Technical settings included power supply stability (mains vs. stabilizer vs. battery) to mitigate source fluctuations, as voltage variations can alter the internal light source intensity and downstream electronics, thereby introducing measurement noise [22]. Data repeatability was also assessed to distinguish true sample characteristics from device drift, ensuring that observed changes were not artifacts of temporal instability [23,24].

Image acquisition parameters were selected to evaluate the trade-offs between file size, color gamut, and signal linearity. We compared Internal Color Management (ICM) profiles, including sRGB, Adobe RGB, and ColorMatch RGB, against manual gamma correction (γ = 1.8 and 2.2) to determine if deactivating the scanner's automatic mapping yields more linear raw data [25]. Output file formats were tested by contrasting lossy JPEG compression, which may introduce artifacts at high compression rates, with lossless TIFF and uncompressed BMP formats preferred for archival precision [26,27]. Furthermore, bit depth was varied between 24-bit (standard) and 48-bit (high dynamic range) to assess if the increased color information (16 bits per channel) significantly improved gradient smoothness and detail retention in the sugar samples [28]. Resolution was also tested across a broad range (50 - 1200 DPI) to identify the optimal balance between detail capture and manageable storage sizes [29, 30].

Regarding sample presentation, physical factors including container dimensions (height and diameter), cover color (black/white/none), and transparent substrate type (e.g., quartz, glass, Plexiglas) were varied. These physical attributes critically influence the optical path length and the degree of diffuse reflection; for instance, a white cover may increase brightness via reflection, while a black cover absorbs scattered light, potentially improving contrast [31]. Similarly, the refractive index and UV-transmission properties of the substrate materials (quartz vs. glass) were evaluated for their impact on the returned light intensity [32].

The scanner's adjustable parameters and the powder sample container's physical attributes were identified as potential variables affecting the data [33]. However, testing the full factorial matrix (over 635,000 combinations) was unfeasible.

Therefore, we employed a fractional and strategic reduction approach: some parameters were held constant while others were systematically varied. This approach ensured feasibility and scientific rigor, allowing for targeted evaluation of influential factors. Factors for variation were chosen based on their relevance to scanner performance and data quality. This structured reduction facilitated manageable testing while enabling the identification of critical effects and interactions, as detailed in table 2, which outlines the constant factors and variables for each experimental scenario.

Table 2. Constant and variable factors across experimental scenarios (abbreviated).

Factors	Tests to investigate							
	1-1	1-2	1-3	1-4	1-5	1-6	1-7	1-8
Power supply	Mains power, Stabilizer, Battery mode of stabilizer	Mains power	Mains power	Mains power	Mains power	Mains power	Mains power	Mains power
Gamma correction	2.2	2.2	1.8, 2.2	2.2	2.2	2.2	2.2	2.2
ICM	off	off	Adobe RGB Apple, RGB ColorMatch, sRGB	off	off	off	off	off
Image format	Tiff	Tiff	Jpg , Tiff, Bmp	Tiff	Tiff	Tiff	Tiff	Tiff
Bit depth	24	24	24	24, 48	24	24	24	24
Resolution(Dpi)	300	300	300	300	50,96,200,300, 600,600, 1200	300	300	300
Surrounding cover	Black	Black	Black	Black	Black	Black	Black, White, White (Leneta), Black(Leneta), None	Black
Tube diameter(cm)	6	6	6	6	6	2, 3,4, 5,6,10	6	6
Tube height(cm)	10	10	10	10	10	0.5,1,2, 3,4, 10	10	10
Substrate	Quartz	Quartz	Quartz	Quartz	Quartz	Quartz	Quartz	Glass, PlexiGlass, Quartz, None

3. Result and Discussion

3.1. The Effect of Power Source

To determine the effect of the power source on the scanner's data, three modes were investigated: using mains electricity (220 V, 50 Hz), using a stabilizer model Alja 3000VA connected to mains electricity, and using the battery mode of stabilizer without connecting to mains electricity. Then, to place the sugar sample on the scanner, a transparent plastic film, shaped into a cylinder with a height of 10 cm and a diameter of 6 cm, and glued onto a 1 mm thick quartz substrate, was prepared. The cylinder was filled with the sugar sample and positioned at a specific location (near the center and the same spot for all measurements) on the scanner's surface (figure 4b).

Also, to prevent the phenomenon of iridescence in the tangential interface between the quartz and the scanner's surface, a 0.5 mm thick black spacer was used. Subsequently, to prevent any potential light from the environment, the entire cylinder was covered with black cardboard (figure 4). For each mode, 10 measurements were taken at 5-minute intervals without changing the sugar sample's position. Other scanner settings were kept constant according to table 2. The average R, G, B channel values obtained from 10 measurements of the sugar sample with the scanner and the statistical results obtained in the three power source modes (mains electricity, stabilizer, and battery mode of stabilizer) are presented in table 3.

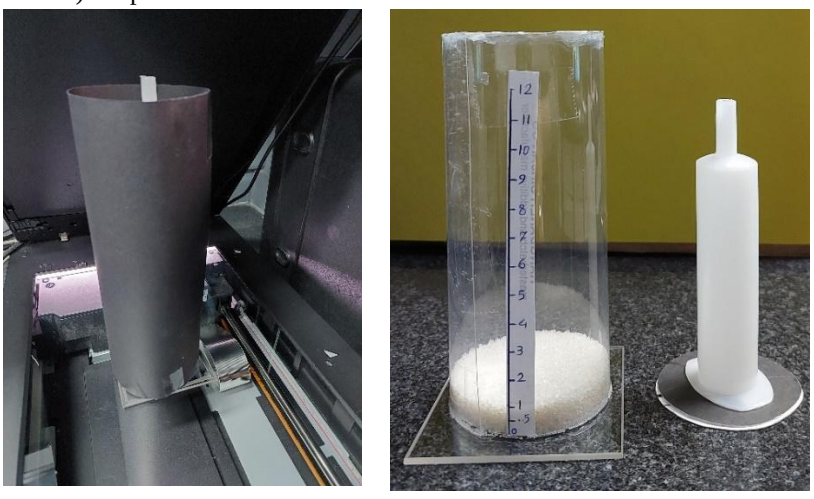

(b)

(a)

Figure 4. (a) Sugar sample in measuring container; (b) container placement on scanner.

Table 3. Statistical results of scanner RGB values under three power modes (Means, STD, CV%).

Mood		R	G	B	AVE
Mains power	MEAN	185.30	182.42	163.82	
	STD	0.027	0.028	0.019	0.0245
	CV%	0.015	0.015	0.012	0.0138
Stabilizer	MEAN	185.16	182.42	163.42	
	STD	0.086	0.129	0.079	0.098
	CV%	0.047	0.071	0.049	0.055
Battery mode of stabilizer	MEAN	185.02	182.35	163.73	
	STD	0.055	0.093	0.171	0.106
	CV%	0.030	0.051	0.104	0.0615

While the type of power supply had a negligible effect on overall color intensity (average R, G, B changes were less than 0.3 units), data stability varied. Mains power yielded the most stable performance, with the lowest standard deviation and coefficient of variation across all RGB channels (average CV% = 0.0138). Conversely, using a stabilizer increased output fluctuations, with some channels showing a five-fold increase in CV% compared to mains power. Battery mode of stabilizer exhibited the highest variability, particularly in the blue channel (CV% = 0.104).

These findings indicate that although battery mode of stabilizer or stabilizer use doesn't alter average color values or introduce systematic error, it can increase noise and reduce measurement repeatability. Given the importance of accuracy and stability in colorimetry and food quality measurement, mains power was selected for the remainder of the research.

3.2. Repeatability Assessment

We assessed scanner data repeatability by measuring a sugar sample's RGB values 10 consecutive times under identical conditions, with 5-minute intervals, after connecting the scanner to mains electricity. The scanner resolution was 300 dpi. Repeatability was evaluated using statistical indices from equations (1)-(5), based on standard sources [34, 35].

$$\text{Variance} \qquad \sigma = \frac{1}{n}\sum_{i=n}^{n}(x_i - \bar{x})^2 \qquad (1)$$

$$\text{Range} \qquad \max(x_i) - \min(x_i) \qquad (2)$$

$$\text{Confidence Interval 95\%} \qquad \bar{x} \pm z\frac{\sigma}{\sqrt{n}} \qquad (3)$$

$$\text{W Shapiro-Wilk, p} \qquad \frac{(\sum_{i=1}^{\frac{n}{2}} a_i\,[x_{(n+1-i)} - x_{(i)}])^2}{\sum_{i=1}^{n}(x_i - \bar{x})^2} \qquad (4)$$

$$\sigma^2\text{=0.01, p} \qquad \frac{\sigma(n-1)}{0.01} \qquad (5)$$

where x_i is the value of each measurement, $\bar{x}$ is the mean of the measurements, and n is the number of measurements. We calculated the variance (spread of the data relative to the mean), the range (difference between the largest and smallest values), and the 95% confidence interval (the range likely to contain the true population mean) using standard formulas. The Shapiro–Wilk test assessed the normality of the measurements, while the chi-

squared test checked whether the observed variance was significantly less than a predefined tolerance limit (p = 0.01). Table 4 presents the R, G, B channel data for 10 sugar sample measurements and their repeatability calculations based on relations 2 to 6.

Table 4. Ten repeated measurements of R, G, and B and repeatability metrics (Variance, Range, CI 95%, Shapiro-Wilk p).

	R	G	B
1	185.32	182.46	163.82
2	185.27	182.40	163.84
3	185.30	182.38	163.80
4	185.25	182.38	163.82
5	185.27	182.41	163.81
6	185.31	182.42	163.83
7	185.28	182.45	163.83
8	185.32	182.43	163.84
9	185.32	182.44	163.79
10	185.32	182.41	163.79
Variance	0.000693	0.000751	0.000357
Range	0.07	0.08	0.05
CI 95%	(185.277 – 185.315)	(182.398 – 182.438)	(163.803 – 163.831)
Shapiro-Wilk, p	0.051	0.730	0.275
σ^2=0.01, p	0.624	0.676	0.321

Table 4 shows high measurement repeatability, with very low sample variances and a small range of values. All channels passed the Shapiro-Wilk normality test (p > 0.05), confirming a normal data distribution. The chi-squared test for variance also indicated negligible variability, as observed variances did not significantly differ from the assumed variance.

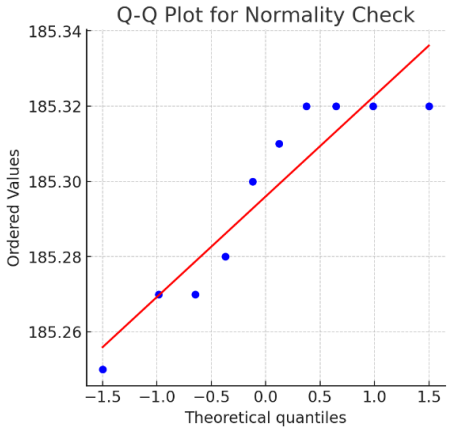

Figure 5. Q–Q plots show data points close to the theoretical normal line, confirming high repeatability.

The data points in figure 5 closely align with the theoretical normal distribution, with only minor deviations at the tails. Statistical analysis confirms the scanner's high repeatability in sugar sample measurements, evidenced by constant means, negligible dispersion, and a CV% under 0.02%. This indicates the scanner produces highly accurate and repeatable color data under consistent experimental conditions.

3.3. The Effect of Gamma Correction, Internal Color Management, and RGB Image Format Type

This scenario examines the impact of gamma correction (1.8 and 2.2), internal color management (Apple RGB, sRGB, Adobe RGB, ColorMatch RGB), and image format (JPEG, TIFF, BMP) on scanner data, with other settings as detailed in table 2. A four-step process was used to convert scanner RGB values to the XYZ color space under

$D_{65}/2^{\circ}$ standard illuminant /observer. First, RGB values were normalized from 0–255 to 0–1. Second, RGB values were linearized using gamma correction specific to each internal color managements: sRGB used its standard transfer function, while Adobe RGB ($\gamma = 2.2$), Apple RGB ($\gamma = 1.8$), and ColorMatch RGB ($\gamma = 1.8$) used their respective power functions. Third, linearized RGB values were converted to XYZ using color-space-specific transformation matrices, then multiplied by 100 to meet standard color measurement conventions[36]. These matrices adhere to CIE and ICC standards for a D_{65} illuminant and a 2° observer. Finally, other color metrics were calculated from the XYZ values, and color differences (ΔE_{00} and ΔE^{*}_{ab}) were measured against spectroradiometric results of the same sugar sample under the specified conditions (table 5).

Table 5. Color differences between spectrophotoradiometer reference and scanner under different ICM, gamma, and image formats.

ICM, Gamma	Format	MeanR	MeanG	MeanB	X	Y	Z	L^{*}	a^{*}	b^{*}	C	h°	ΔE^{*}_{ab}	ΔE_{00}
AdobeRGB	BMP	204.89	202.06	190.03	56.61	59.92	57.80	81.79	-0.83	6.67	6.72	97.11	9.53	6.96
	JPEG	204.44	202.38	190.27	56.51	59.97	57.95	81.82	-1.21	6.58	6.69	100.45	9.69	7.23
	TIFF	204.94	201.87	189.88	56.59	59.84	57.70	81.75	-0.71	6.69	6.73	96.03	9.47	6.87
AppleRGB	BMP	196.43	191.81	176.77	56.60	59.86	57.73	81.76	-0.73	6.68	6.72	96.21	9.49	6.89
	JPEG	196.72	191.78	177.46	56.74	59.92	58.07	81.79	-0.53	6.42	6.44	94.70	9.65	6.95
	TIFF	196.17	191.88	176.78	56.54	59.84	57.73	81.75	-0.83	6.66	6.71	97.12	9.51	6.95
ColorMatchRGB	BMP	195.67	191.88	176.67	57.78	59.97	43.78	81.82	1.90	21.04	21.13	84.83	11.17	7.07
	JPEG	195.49	191.89	177.33	57.77	59.97	44.02	81.82	1.90	20.78	20.86	84.79	10.97	6.98
	TIFF	195.37	191.94	176.43	57.68	59.94	43.69	81.80	1.75	21.11	21.18	85.26	11.20	7.07
sRGB	BMP	207.07	203.25	190.80	56.55	59.86	57.74	81.76	-0.86	6.67	6.73	97.32	9.51	6.96
	JPEG	206.84	203.61	191.35	56.63	60.02	58.08	81.85	-1.03	6.50	6.58	99.03	9.72	7.17
	TIFF	206.99	203.18	190.73	56.50	59.81	57.69	81.74	-0.86	6.67	6.73	97.37	9.49	6.95
Gamma 1.8	BMP	170.20	166.98	145.75	43.20	46.28	41.22	73.73	-2.33	10.03	10.29	103.05	4.14	4.56
	JPEG	170.44	167.16	145.54	43.27	46.37	41.14	73.78	-2.37	10.21	10.48	103.05	4.05	4.55
	TIFF	170.15	166.97	145.66	43.18	46.27	41.18	73.72	-2.35	10.06	10.33	103.17	4.15	4.59
Gamma 2.2	BMP	183.06	180.47	161.63	43.22	46.33	41.36	73.76	-2.39	9.92	10.20	103.58	4.26	4.68
	JPEG	182.70	180.70	161.62	43.18	46.38	41.36	73.79	-2.65	9.97	10.31	104.90	4.42	4.97
	TIFF	182.93	180.33	161.49	43.15	46.25	41.28	73.71	-2.39	9.92	10.20	103.55	4.26	4.68

The results presented in table 5 indicate that among all scanner settings, lightness values in the CIELAB color space were relatively stable, ranging from approximately 73.71 to 81.85. This stability suggests that imaging with the scanner can accurately record the lightness information of sugar samples. However, the red/green component a^{*} and the blue/yellow component b^{*}, as well as derived parameters like chroma C^{*} and hue angle h°, showed greater fluctuations, especially in the ColorMatchRGB profile where chroma values were significantly higher (e.g., $C^{*} \approx 21$, while under Adobe RGB and sRGB profiles $C^{*} \approx 6.7$). Gamma settings also had a notable impact on color characteristics: Gamma 1.8 profiles produced higher b* and chroma values, indicating increased yellow–blue contrast, while Gamma 2.2 profiles slightly reduced chroma but increased the hue angle.

To assess the deviation of the scanner-obtained color values from the spectrophotometric reference, the color difference indices ΔE^{*}_{ab} and ΔE_{00} were used. All profiles related to the scanner's internal color management, regardless of image format, resulted in the highest color difference values ($\Delta E_{00} \approx 6.87$–$7.23$). In contrast, gamma-correction-based profiles yielded the lowest ΔE_{00} values ($\Delta E_{00} \approx 4.557$–$4.97$), demonstrating the strong potential of gamma correction for more accurate color reproduction. An examination of image formats also shows that, in general, TIFF produces lower ΔE_{00} values compared to JPEG and BMP, indicating that lossless formats better preserve color information.

3.4. The Effect of Bit Depth.

In this scenario, fixed factors were selected according to table 2, and then color data of sugar samples were recorded using an RGB scanner in two different bit depth modes (24-bit and 48-bit) and two gamma correction modes ($\gamma = 1.8, 2.2$). 24-bit image data is typically stored as uint8 arrays, where each color channel (red, green, blue) has a numerical range between 0 and 255. In contrast, 48-bit data is stored as uint16, with each channel having a numerical range between 0 and 65535.

After detecting the bit depth, the RGB data was converted to double type and normalized to the range [0, 1] using an appropriate scaling factor (255 for uint8 data and 65535 for uint16 data). Then, the normalized data was converted to XYZ and subsequently to other color values using the corresponding specific transformation table.

Table 6. Comparison of 24-bit and 48-bit scans (mean RGB, XYZ, L^*, a^*, b^*, ΔE_{00}).

Name	MeanR	MeanG	MeanB	X	Y	Z	L*	a*	b*	C*	h°	ΔE^*_{ab}	ΔE_{00}
24bit,1.8 Gamma	169.94	166.76	145.33	43.07	46.16	41.02	73.65	-2.37	10.12	10.40	103.19	4.14	4.60
24bit, 2.2 Gamma	189.15	185.01	164.25	45.89	49.07	42.99	75.5	-2.14	11.02	11.23	100.97	3.47	4.07
48bit,1.8 Gamma	43555.65	42738.09	37306.30	42.88	45.94	40.92	73.51	-2.33	10.00	10.27	103.12	4.22	4.60
48bit, 2.2 Gamma	46868.66	46166.88	41347.85	42.82	45.88	40.94	73.47	-2.33	9.90	10.17	103.24	4.29	4.64

Results (table 6) showed that increasing bit depth has a negligible effect on colorimetric parameters. 48-bit data yielded L^*, a^*, b^* values and color differences nearly identical to 24-bit results, indicating that for the measurement sugar sample, 24-bit with proper gamma correction offers sufficient color accuracy. Slight variations in ΔE_{00} (4.07 to 4.64) are mainly attributed to gamma correction differences, not bit depth. A gamma setting of 2.2 generally leads to lower ΔE_{00} values.

3.5. The Effect of Resolution

In this scenario, the sugar sample was measured at resolutions from 50 (resolution floor) to 1200 dpi, with other factors held constant (table 2). Results (table 7) showed that 300 dpi is optimal due to its good image quality and reasonable scan time (18 seconds), as ΔE values were very similar across resolutions. Higher resolutions, such as 1200 dpi, significantly increased processing time (2 minutes 40 seconds).

Table 7. Color differences and scan times at different resolutions.

Resolution	MeanR	MeanG	MeanB	X	Y	Z	L^*	a^*	b^*	C^*	h°	ΔE^*_{ab}	ΔE_{00}	$Time_{(s)}$
50	182.89	180.23	161.40	43.11	46.20	41.23	73.68	-2.37	9.93	10.21	103.41	4.25	4.65	12
96	182.71	180.11	161.31	43.04	46.13	41.18	73.63	-2.39	9.90	10.19	103.55	4.29	4.69	13
200	181.88	179.36	160.71	42.63	45.70	40.83	73.35	-2.39	9.83	10.12	103.68	4.41	4.76	16
300	182.82	180.11	161.27	43.06	46.14	41.16	73.64	-2.35	9.94	10.21	103.31	4.24	4.63	19
600	183.37	180.89	161.80	43.40	46.55	41.47	73.90	-2.48	10.03	10.33	103.88	4.23	4.73	30
800	183.69	180.60	161.60	43.40	46.46	41.36	73.84	-2.24	10.06	10.31	102.54	4.04	4.44	59
1200	183.40	180.21	161.37	43.23	46.26	41.22	73.71	-2.18	10.00	10.23	102.29	4.06	4.40	164

Table 7 indicates that increased resolution had a negligible impact on the sugar sample's colorimetric parameters. L^*, a^*, b^* values, and chroma remained stable from 50 to 1200 dpi, with ΔE_{00} varying only slightly (4.40 to 4.76). This suggests that resolutions above 300 dpi do not substantially improve color accuracy; minor ΔE fluctuations are likely due to systematic errors. Conversely, scanning time increased exponentially with resolution (12 to 164 seconds) without significantly reducing color differences. Thus, optimal resolution settings are 300-600 dpi, offering measurement times of 30 to 60 seconds.

3.6. The Effect of Height, Diameter, and Type of Cover of Sugar Sample Container

In this scenario, we investigated the impact of container height (0.5-10 cm), diameter (2-10 cm), and cover type (black cardboard, standard white and black cardboard (Lenta paper), ordinary white cardboard containing fluorescent materials, and without covering) on sugar sample color difference. This involved 140 measurements. A full factorial design, analyzed using a three-way ANOVA with a reduced model (main effects and two-way interactions), evaluated how these factors influence the color difference between a sugar sample and a reference sample. The model, fitted using the least squares method, was:

$$\Delta E_{00} \sim \text{Cover} + \text{Diameter} + \text{Height} + \text{Cover}\times\text{Diameter} + \text{Cover}\times\text{Height} + \text{Diameter}\times\text{Height}$$

Residual plots confirmed normality and homogeneity of variance, allowing for comparisons of two-way interactions to identify significant effects. The ANOVA table (Type II sum of squares) is provided below:

Table 8. Three-way analysis of variance (ANOVA) based on the reduced model including main effects and two-way interactions.

Source	Sum of Squares	df	F	p-value
Cover	8.9899	3	123.78	<0.001
Diameter	15.0825	4	155.75	<0.001
Height	1.0092	6	6.95	<0.001
Cover × Diameter	6.1339	12	21.11	<0.001
Cover × Height	0.2785	18	0.64	0.856
Diameter × Height	0.9749	24	1.68	0.048
Residual	1.7430	72	-	-

Table 8 demonstrates that cover type and container diameter are the most influential factors affecting ΔE_{00}, the perceptual color difference between scanner and spectrophotometer measurements of sugar. A three-way ANOVA confirmed significant effects for cover type ($F(3,72) = 123.78$, $p < 0.001$), container diameter ($F(4,72) = 155.75$, $p < 0.001$), and sample height ($F(6,72) = 6.95$, $p < 0.001$). The interaction between cover type and diameter was also highly significant ($F(12,72) = 21.11$, $p < 0.001$), indicating that the effect of the cover varies with diameter. The diameter × height interaction was marginally significant ($F(24,72) = 1.68$, $p = 0.048$), while the cover × height interaction was not ($F(18,72) = 0.64$, $p = 0.856$).

None-cover containers and those with ordinary fluorescent cardboard covers resulted in the highest average ΔE_{00} values (5.55 and 5.54, respectively), likely due to fluorescent, light scattering or edge effects. In contrast, the white, fluorescent-free cover performed best (average $\Delta E_{00} = 4.94$). It seems the white cover mimics the infinite optical thickness of a deep sugar container, preventing 'graying' caused by light escaping through the translucent crystals into a black background. Increasing container diameter consistently reduced ΔE_{00} (from 5.80 at 2 cm to 5.06 at 6 cm). Sample height also had a moderate, consistent effect, with ΔE_{00} decreasing slightly from 5.57 at 0.5 cm to 5.30 at 10 cm. The significant cover × diameter interaction highlights the benefit of white cover for medium-diameter containers (e.g., $\Delta E_{00} \approx 4.72$ at 5 cm), optimizing scanner-based colorimetry for low-volume sugar analysis. In conclusion, white Lenta cardboard cover and diameters ≥4 cm are optimal, yielding a $\Delta E_{00} < 5$.

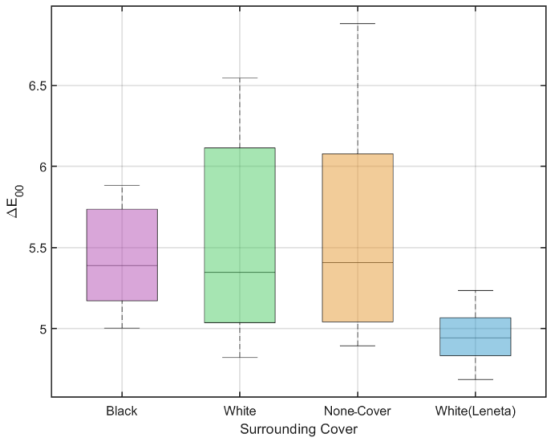

Figure 6. ΔE_{00} vs cover type (boxplot).

Figure 6 shows that covering the measuring container with non-fluorescent white cardboard(Lenta cardboard) yielded the lowest median ΔE_{00} value (4.8), indicating the least color difference from spectrophotometer data. The black covering also showed a relatively low median dispersion of 5.5. Conversely, ordinary fluorescent white cardboard and no covering both resulted in higher median ΔE_{00} values (around 6) and increased dispersion, leading to greater color differences.

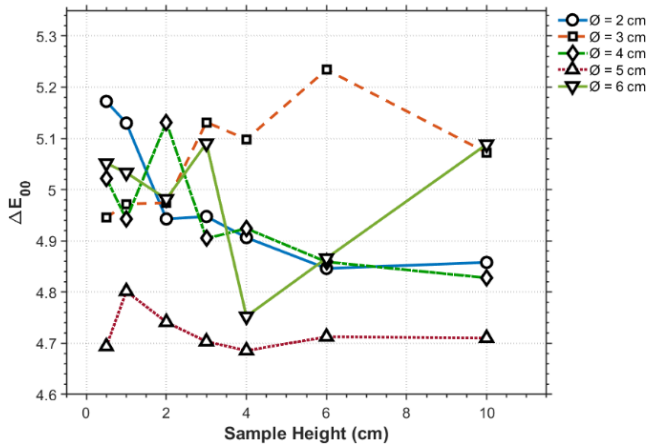

Figure 7. ΔE₀₀ between sugar samples and the reference as a function of sample height for different diameters(Ø).

Figure 7 shows the ΔE₀₀ generally decreases with increasing sample height up to approximately 4–6 cm, after which further height increases provide little or no additional benefit in most cases. The lowest and most stable color differences (ΔE₀₀ ≈ 4.70–4.85) are consistently achieved with the largest container diameters (Ø = 5 cm and Ø = 6 cm) at heights ≥ 4 cm. Smaller container diameters (Ø = 2–3 cm) show higher and more variable ΔE₀₀ values, particularly at low heights, most likely due to stronger edge and boundary effects. These results indicate that a combination of sample height ≥ 4 cm and diameter ≥ 5 cm is optimal for minimizing colorimetric deviation in this measurement configuration.

3.7. The Effect of transparent substrate

For optimal color-sensitive imaging of sugar samples, a transparent substrate is required between the sample and the scanner plate. We evaluated glass, plexiglass, quartz, and direct placement (no substrate). Glass was a German Petri dish; quartz and plexiglass were 1mm in diameter, with plexiglass being scratch-free. Spectral transmission (400–700 nm) of these three substrates measured in transmission mode (n = 3 per material) and plotted as triplicate mean after 10 nm resampling and smoothing by spectrophotometer.

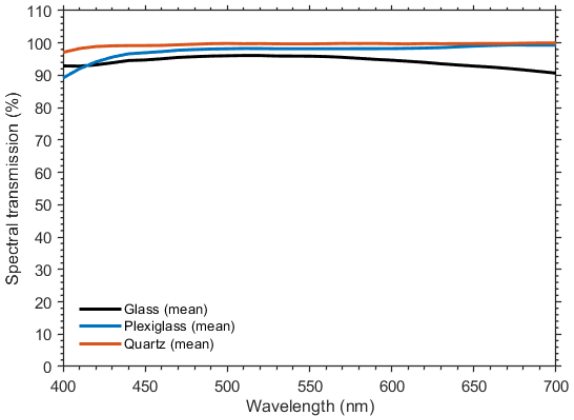

Figure 8. The spectral transmition of three transparent substrates (Glass, Plexiglass and Quartz).

Figure 8 shows the Quartz exhibits the highest and most spectrally uniform visible transmission, consistent with minimal absorption in the 400–700 nm range. Plexiglass and glass show lower transmission with stronger wavelength dependence, indicating comparatively higher attenuation and material specific spectral losses.

Table 9 presents color values and color differences (ΔE^*_{ab} and ΔE₀₀) with spectrophotometric data. For direct placement, the sugar sample was placed in a plastic tube directly on the scanner.

Table 9. Color differences for different substrates of sample container.

Substrate	L^*	a^*	b^*	C^*	h°	ΔE^*_{ab}	ΔE_{00}
Non Substrate	79.53	-1.72	11.63	11.75	98.41	5.69	4.90
Glass	74.07	-4.07	10.01	10.81	112.14	5.55	6.64
PlexiGlass	74.11	-2.10	10.59	10.80	101.22	3.57	4.09
Quartz	75.26	-2.16	10.34	10.56	101.78	3.81	4.25

The results show that in the Non-substrate (direct-contact) configuration, the sample exhibits the highest lightness $L^* = 79.53$ and a smaller green shift $a^* = -1.72$, while maintaining a comparatively high yellowness $b^*=11.63$. This is consistent with reduced transmission losses when no interface is introduced, although direct coupling to the scanner window can increase stray-light and specular effects, subtly altering the a^*/b^* balance and contributing to the remaining ΔE. Also quartz and plexiglass substrates caused less color difference between scanner and spectrophotometer data compared to glass. Quartz, with ΔE_{00} values similar to direct contact, proved ideal for color-sensitive imaging. While plexiglass showed the lowest ΔE^*_{ab} and ΔE_{00} values, its optical properties can vary. Therefore, quartz was selected as the optimal substrate due to its transparency, spectral neutrality, and availability.

3.8. Comparison with Emerging Computer Vision Technologies

While recent advancements have introduced AI-driven computer vision and smartphone colorimetry as flexible tools for food quality assessment [37, 38], these open-system approaches often struggle with illumination consistency compared to the controlled environment of a flatbed scanner. For instance, other investigation reported that direct smartphone-based RGB colorimetry yielded a mean color difference ΔE^* of 8.2, with deviations exceeding 20 units in complex scenarios, which is significantly higher than the $\Delta E_{00} \approx 4.07$ achieved in this study [39]. This confirms that for white powdered foods such as sugar, where subtle whiteness indices are critical, the fixed geometry and stable lighting of an optimized flatbed scanner provide superior repeatability over handheld mobile solutions.

Finally, it is important to clarify the scope of these optimization results. We deliberately focused on tuning the instrument rather than characterizing a wide variety of samples. The optimal settings identified here, such as mains power for stability, Gamma 2.2 for linearity, and quartz for transparency, are determined by the scanner's opto-electronics and physical laws, which remain constant regardless of the sugar sample. By using a single, stable sugar sample as a reference(through spectrophotometry), we could isolate and minimize instrumental errors. Now that the scanner's physical baseline is established, future research can apply these fixed settings to develop robust calibration models across a broad spectrum of commercial sugars.

4. Conclusion

The results of this study showed that a digital scanner, when properly adjusted and corractrized for technical parameters and physical specifications of the container holding white powdered samples such as sugar, can reduce the perceived color difference from 7.23 to 4.07 compared to data obtained through a spectrophotometer. Among the variables examined under these specific conditions, mains power supply, using RGB values with gamma correction of 2.2, uncompressed image format (TIFF), and medium resolution (300-600 dpi) yielded the closest color difference to reference data. The results also indicated that the height and diameter of the sample in the container and the container cover type significantly impact the color difference, such that using a container with a 4 cm diameter and a non-fluorescent white cover reduces the color difference to less than 5 ΔE_{00} units. While these preliminary optimization results suggest that flatbed scanners hold potential as relatively accurate, cost-effective, and reliable tools for evaluating the color of white and powdered food materials, the method does not yet achieve the high precision required for industrial trading standards $\Delta E_{00} < 2$. In future work, subsequent validation phases will include a diverse range of sugar grades and particle sizes to verify the global robustness of the optimized parameters. Furthermore, the study should extend this parameter optimization across a wider variety of powdered

materials with different scattering and absorption properties and evaluate multi-device cross-calibration strategies. However, to achieve even smaller color difference values compared to spectrophotometric results, it is necessary to identify an effective non-linear conversion of RGB to XYZ.

Acknowledgment

The authors would like to express their sincere gratitude to the Institute for Color Science and Technology for providing the necessary facilities and technical support for the measurements. The authors also extend their appreciation to the Qazvin Sugar Factory for kindly supplying the sample used in this study.

Author Contributions Keivan Ansari: Conceptualization, Formal analysis, Methodology, Project administration, Software, Supervision, Writing – original draft. Leila Ziafar: Investigation, Data curation, Formal analysis, Resources, Writing – review & editing. Masoud Honarvar: Conceptualization, Supervision, Resources, Data curation, Project administration, Writing – review & editing. Vahid Mohammadi: Conceptualization, Formal analysis, , Assistance in validation, Visualization, Assistance in validation, Writing – review & editing.

Funding This work received no funding.

Data availability Data will be made available on request.

Declarations

Conflict of interest The authors declare no conflict of interest.

Refrences

[1] Bahrami M E, Honarvar M, Ansari K and Jamshidi B 2020 Measurement of quality parameters of sugar beet juices using near-infrared spectroscopy and chemometrics *J. Food Eng.* 271 109775 (doi: 10.1016/j.jfoodeng.2019.109775)

[2] Gratton L M, López-Arias T, Calzà G and Oss S 2009 The whiteness of things and light scattering Phys. Educ. 44 411 (doi: 10.1088/0031-9120/44/4/011)

[3] Zhao K, Zhang M, Ji J, Sun J and Ma H 2023 Whiteness measurement of Agaricus bisporus based on image processing and color calibration model *Food Measure* 17 2152–61 (doi: 10.1007/s11694-022-01748-w)

[4] Martinez-Velasco J D, Filomena-Ambrosio A and Garzón-Castro C L 2024 Technological tools for the measurement of sensory characteristics in food: A review *F1000 Research* 12 340 (doi: 10.12688/f1000research.131914.2)

[5] Bahrami M E and Ansari K 2015 *6th Int. Color and Coating Congress (ICCC)* (Tehran, Iran, 10-12 November)

[6] Milovanovic B, Tomovic V, Djekic I, Solowiej B J, Lorenzo J M, Barba F J and Tomasevic I 2021 Color assessment of the eggs using computer vision system and Minolta colorimeter *Food Measure* 15 5097–112 (doi: 10.1007/s11694-021-01085-4)

[7] Lee B-S, Bala R and Sharma G 2006 *Proc. SPIE 6065* 606512 (doi: 10.1117/12.658634)

[8] Kangasrääsiö J and Hemming B 2009 Calibration of a flatbed scanner for traceable paper area measurement Meas. Sci. Technol. 20 107003 (doi: 10.1088/0957-0233/20/10/107003)

[9] Brosnan T and Sun D-W 2004 Improving quality inspection of food products by computer vision, a review *J. Food Eng.* 61 3–16 (doi: 10.1016/S0260-8774(03)00183-3)

[10] Hani O E, Digua K and Amine A 2025 On-site saffron origin identification using image processing and chemometric tools *Food Measure* 19 6802–14 (doi: 10.1007/s11694-025-03414-3)

[11] Bahrami M E, Honarvar M and Ansari K 2017 Feasibility of Using Digital Image Processing and Colorimetric Measurements to Estimate the Physicochemical Properties of Raw Cane Sugars *Sugar Tech* 19 305–16 (doi: 10.1007/s12355-016-0467-5)

[12] Togban E and Ziou D 2025 Improved image display by identifying the RGB family color space *Displays* 90 102587 (doi: 10.1016/j.displa.2024.102587)

[13] Lee Y-K, Yu B, Lee S-H, Cho M-S, Lee C-Y and Lim H-N 2010 Variation in instrument-based color coordinates of esthetic restorative materials by measurement method-a review *Dent. Mater.* 26 1098–105 (doi: 10.1016/j.dental.2010.07.010)

[14] Horibe T, Ishii K, Fukutomi D and Awazu K 2015 Influence of diffuse reflectance measurement accuracy on the scattering coefficient in determination of optical properties with integrating sphere optics (a secondary publication) *Laser Ther.* 24 303–10 (doi: 10.5978/islsm.15-OR-19)
[15] Institute of Standards and Industrial Research of Iran (ISIRI) 2018 Sugar - White sugar - Specifications and test methods ISIRI Standard No. 69
[16] Codex Alimentarius Commission 1999 Standard for Sugars CODEX STAN 212-1999 (Amd. 1-2001)
[17] International Commission for Uniform Methods of Sugar Analysis (ICUMSA) 2007 Particle size distribution of white sugar by sieving Method GS2/9-37
[18] Goñi S M and Salvadori V O 2017 Color measurement: comparison of colorimeter vs. computer vision system *Food Measure* 11 538–47 (doi: 10.1007/s11694-016-9421-1)
[19] Laddi A, Prakash N R, Sharma S and Kumar A 2013 Discrimination analysis of Indian tea varieties based upon color under optimum illumination *Food Measure* 7 60–5 (doi: 10.1007/s11694-013-9139-2)
[20] Mohammadi V, Ansari K, Gouton P and Attig H 2024 Developing a new method of transformation for obtaining XYZ color values from RGB images for agricultural applications *Sensors* 24 7728 (doi: 10.3390/s24237728)
[21] Cruz-Bernal A, León-Rodríguez M, Rodríguez-Ponce R, Ibarra-Torres P, Muñoz F G-M, and Méndez G G 2024 Physicochemical quality visual characterization postharvest of bell pepper applying recent mathematics techniques in the digital image processing *Food Measure* 18 9078–85 (doi: 10.1007/s11694-024-02860-9)
[22] Nocoń and Paszek S 2023 A comprehensive review of power system stabilizers *Energies* 16 1945 (doi: 10.3390/en16041945)
[23] Goldstein G R and Schmitt G W 1993 Repeatability of a specially designed intraoral colorimeter *J. Prosthet. Dent.* 69 616–9 (doi: 10.1016/0022-3913(93)90258-5)
[24] Hasanlou E, Shams Nateri A and Izadan H 2022 The effect of scanner resolution and bit depth on measuring color changes of fabric in small color space *J. Color Sci. Technol.* 16 123–34 (DOR: 20.1001.1.17358779.1401.16.2.3.7)
[25] Soni S, Singh P and Waoo A 2024 Review of gamma correction techniques in digital imaging *ShodhKosh J. Vis. Perform. Arts* 5 1075–84 (doi: 10.29121/shodhkosh.v5.i5.2024.1902)
[26] Alfio V S, Costantino D and Pepe M 2020 Influence of image TIFF format and JPEG compression level in the accuracy of the 3D model and quality of the orthophoto in UAV photogrammetry *J. Imaging* 6 30 (doi: 10.3390/jimaging6050030)
[27] Ungureanu V I, Negirla P and Korodi A 2024 Image-compression techniques: Classical and region-of-interest-based approaches presented in recent papers *Sensors* 24 791 (doi: 10.3390/s24030791)
[28] Mahbod A, Schaefer G, Löw C, Dorffner G, Ecker R and Ellinger I 2021 Investigating the impact of the bit depth of fluorescence-stained images on the performance of deep learning-based nuclei instance segmentation *Diagnostics* 11 967 (doi: 10.3390/diagnostics11060967)
[29] Hu Z, Bauer P, Harris T and Allebach J 2021 *IS&T Int. Symp. Electron. Imaging 2021: Color Imaging XXVI-Displaying, Processing, Hardcopy, and Applications* pp 117-1–6 (doi: 10.2352/EI.2021.26.17.COLOR-2021-02)
[30] Minz P S, Sawhney I K and Saini C S 2018 Algorithm for automatic calibration of color vision system in foods *Food Measure* 12 1787–94 (doi: 10.1007/s11694-018-9794-4)
[31] Lewis D and Chan M F 2015 Correcting lateral response artifacts from flatbed scanners for radiochromic film dosimetry *Med. Phys.* 42 416–29 (doi: 10.1118/1.4903758)
[32] Yusufu D and Mills A 2018 Spectrophotometric and digital colorimetric (DCC) analysis of colour-based indicators *Sens. Actuators B Chem.* 273 1187–94 (doi: 10.1016/j.snb.2018.06.131)
[33] Emady H N, Wittman M, Koynov S, Borghard W G, Muzzio F J, Glasser B J and Cuitino A M 2015 A simple color concentration measurement technique for powders *Powder Technol.* 286 392–400 (doi: 10.1016/j.powtec.2015.07.050)
[34] Montgomery D C 2020 *Introduction to Statistical Quality Control* 8th edn (Wiley)
[35] Heckert N, Filliben J, Croarkin C, Hembree B, Guthrie W, Tobias P and Prinz J 2002 *Handbook 151: NIST/SEMATECH e-Handbook of Statistical Methods* (NIST/SEMATECH) (doi: 10.18434/M32189)
[36] Lindbloom B n.d. RGB/XYZ Matrix Equations (available at: http://www.brucelindbloom.com/index.html?Eqn_RGB_XYZ_Matrix.html) (accessed: 18 February 2026)
[37] Kumar R, Kumar Y, Arora N and Gupta R P 2026 Computer vision technologies for food quality and safety assurance: Evaluating trends and analytical results Food Anal. Methods 19 106 (doi: 10.1007/s12161-026-03019-6)
[38] Shehzad K, Ali U and Munir A 2025 Computer vision for food quality assessment: advances and challenges Glob. J. Mach. Learn. Comput. 1 76–92 (doi :10.70445/gjmlc.1.1.2025.76-92)
[39] Ciaccheri L, Adinolfi B, Mencaglia A A and Mignani A G 2023 Smartphone-enabled colorimetry: A case of study for water quality monitoring Sensors 23 5559 (doi: 10.3390/s23125559)